Assessing the corrosion behaviour of Nitinol for minimally-invasive device design

R. Venugopalan[1] and C. Trépanier[2]

[1]Department of Biomedical Engineering, University of Alabama at Birmingham, Birmingham, AL; and [2]Cordis Corporation – Nitinol Devices and Components, Fremont, CA, USA

Summary

Nitinol is a very attractive material for manufacturing minimally-invasive therapy devices and tools because of its unique superelasticity and shape-memory properties. While several studies have shown it to possess good biocompatibility, its high nickel content and possible dissolution during corrosion still remain a concern. However, passivation and electropolishing can significantly decrease nickel dissolution from Nitinol by forming a corrosion-resistant titanium oxide surface layer. In general, passivated and electropolished Nitinol exhibits equivalent, if not better, static corrosion behaviour and ability to resist and repassivate (repair) surface damage when compared with 316L stainless steel (SS). Combining Nitinol with SS, titanium and tantalum does not significantly affect its corrosion behaviour. However, combining Nitinol with gold, platinum and platinum–iridium alloy can result in an order of magnitude increase in corrosion rate. Nickel release from Nitinol decreases from well below dietary levels to nearly non-detectable levels in the first few days following immersion in a physiological medium. Finally, in vivo studies indicate minimal corrosion of Nitinol during implantation, with released nickel concentration in surrounding tissues or organs being equivalent to that released by 316L SS.

Keywords

Nitinol, passivated, corrosion, scratch-resistance, galvanic

Introduction

Nitinol (NiTi) is a very attractive material for minimally-invasive therapy since it possesses unique mechanical properties (superelasticity and shape-memory) and good biocompatibility [1]. In the last two decades, NiTi technology has contributed to significant improvements in orthopaedics and orthodontics [2,3]. Its use is now overcoming the limits in designing smaller, more efficient minimally-invasive tools and devices [4].

Although several studies have demonstrated the good corrosion resistance and biocompatibility of NiTi, the high nickel content of the alloy (55 weight %

Ni) and its possible dissolution by corrosion still remains a concern [5–9]. Tissues in the human body contain water, dissolved oxygen, proteins and various ions, such as chloride and hydroxide, and they present an aggressive environment to metals or alloys used for implantation [10,11]. Thus, every base-metal/alloy implanted in the body will corrode — the only question is to what extent?

Corrosion resistance of a metallic implant is thus an important aspect of its biocompatibility [12]. In addition to the release of ions in the physiological environment, the corrosion process will also result in the deterioration of dimensional parameters of the

corroding body [13]. While large orthopaedic implants, such as total hips and knees very rarely lose mechanical integrity purely due to corrosion fatigue, small and complex-geometry minimally-invasive devices can be susceptible to failure due to mechanically-assisted corrosion. Thus, when choosing a material for manufacturing minimally-invasive devices, evaluation and optimisation of the corrosion properties should be performed on samples representative of the actual device surface finish or, preferably, the device itself.

NiTi corrosion behaviour can be significantly improved after specific surface treatments such as electropolishing [14]. Not surprisingly, similar surface treatments are prescribed by the American Society for Testing and Material (ASTM) to optimise the corrosion properties of stainless steel (SS) and other biomaterials (F86 standard) [15]. Electropolishing of NiTi homogenises the thickness, topography and chemical composition of the surface layer by forming predominantly titanium oxide — a significant factor in improving corrosion resistance [16,17].

Most minimally-invasive devices are susceptible to surface damage during their manipulation. Such damage can disrupt the surface layer and lead to significantly increased corrosion. Thus, the ability of the device to repair surface damage has to be ascertained, in addition to determining the device's static corrosion behaviour. Finally, galvanic corrosion may occur when dissimilar metals are coupled to NiTi. Indeed, different material devices could be placed in close proximity, or a device may even be made from more than one material to take advantage of their specific properties. An example of the latter case is the use of noble metal markers on SS or Nitinol devices, to improve radiopacity.

Based on these considerations, the objectives of this paper are to:

- discuss *in vitro* static corrosion behaviour and repassivation ability of passivated NiTi in comparison with 316L SS;
- discuss the *in vitro* galvanic corrosion behaviour of passivated NiTi in combination with other biomaterials;
- review prior research on nickel dissolution *in vitro,* and *in vivo* corrosion of NiTi.

In vitro corrosion resistance of NiTi

Potentiodynamic polarisation testing was conducted on electropolished NiTi and 316L SS discs to determine their individual corrosion behaviour under static conditions in Hank's solution [18]. A generic schematic of the experimental configuration used for corrosion testing is shown in Figure 1. After an hour of equilibration, polarisation data was generated by conducting a forward scan from 100 mV more active than the corrosion potential (E_{corr}) to a threshold anodic current density of 10 mA cm^{-2}. The scan direction was reversed until the protection potential was achieved, or the potential was 0 mV with reference to the E_{corr}. Tafel extrapolation, and Stern–Geary currents were used to calculate the corrosion current density (I_{corr}) in A cm^{-2} at the (ParCalc® Routine, Technical Notes/Software Manual, EG&G, Princeton Applied Research). The corrosion rate in mm/year (CR) was calculated based on equivalent weight and density values included in the experimental set-up for the M352 software. The breakdown potential (E_{bd}) was determined from the y axis co-ordinate corresponding to the intersection of a line-fit extrapolation of the passive and transpassive regions.

The E_{corr} is an indicator of the stability of surface conditions. Thus, less variability in E_{corr} values from different samples is indicative of more consistent surface processing. The I_{corr} and calculated CR are
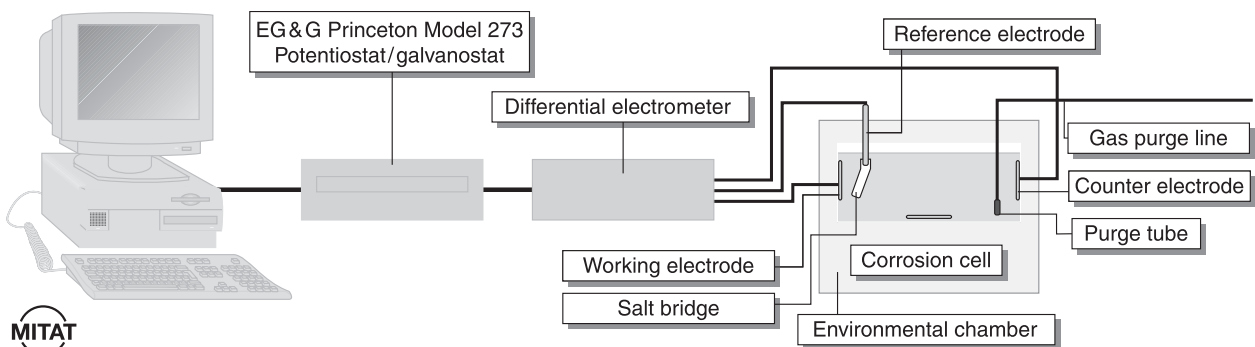

Figure 1. Generic schematic of experimental configuration used for corrosion testing.

relative measures of corrosion and illustrate how much of a material will be lost during the corrosion process. Hence, the higher the I_{corr} and calculated CR, the more the material lost. The E_{bd} is a measure of the region over which a surface layer is stable and corrosion resistant. Thus, a higher or more positive value of E_{bd} would indicate a larger region of corrosion resistance.

The calculated E_{corr}, I_{corr}, CR and E_{bd} values are shown in Table 1. Representative potentiodynamic polarisation plots for NiTi and SS are presented in overlaid format in Figure 2. The E_{corr} for NiTi was more active than for SS. The I_{corr} was very consistent and in the nA cm^{-2} range for both NiTi and SS. The CR values also exhibited no significant difference between SS and NiTi. The E_{bd} for NiTi was almost three times greater than SS. Prior research by Trépanier *et al.* [14] and Rondelli [19] on comparative corrosion behaviour of surface-modified NiTi also presented similar corrosion rates and breakdown potentials. NiTi exhibited instantaneous repassivation on the reverse scan, while SS exhibited a significant hysteresis. Hence, the SS was more susceptible to propagation of existing surface damage than NiTi.

In order to determine their repassivation ability, NiTi and SS discs immersed in Hank's media were scratched using a diamond stylus across the whole exposed diameter 5 min before 0, 200, 400 and 600 mV potentiostatic holds [18]. The current flow during each 15 min potentiostatic hold was monitored and normalised to sample surface area to obtain current density measurements. An asymptotically decreasing current-density trend indicated that the material was able to repassivate the scratch damage at that potentiostatic hold. An increasing current density trend indicated that the sample was not able to repassivate scratch damage at that potentiostatic hold. Current density >500 μA cm^{-2} was used at a threshold value to define total loss of ability of the material to repassivate [20].

Representative current-density curves at 0, 200, 400 and 600 mV potentiostatic holds are presented in overlaid format in Figures 3a–3d. NiTi and SS exhibited asymptotically decreasing current
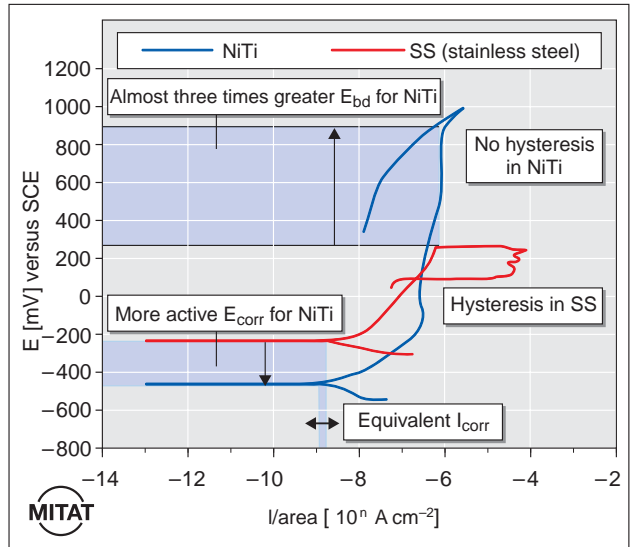

Figure 2. Representative cyclic polarisation curves for NiTi and SS in de-aerated Hanks solution at 37°C. Note the equivalent corrosion rate and the larger passive or corrosion resistant region exhibited by NiTi.

densities and repassivation after scratch damage at the 0 mV potentiostatic hold. NiTi exhibited asymptotically-decreasing current densities and repassivation at the 200 mV potentiostatic hold. While the SS exhibited increasing current densities, it still did not exceed the 500 μA cm^{-2} current density threshold value. This behaviour was indicative of a relatively less-stable passive behaviour by SS compared with NiTi at the 200 mV potentiostatic hold. At the 400 and 600 mV potentiostatic holds, both NiTi and SS exhibited increasing current densities that exceeded the 500 μA cm^{-2} threshold value; indicative of total breakdown of passive layer. It should be noted that SS exhibited a faster current density transient past the 500 μA cm^{-2} threshold value and a couple of orders of magnitude higher corrosion rate than NiTi (Figures 3c and 3d). Thus, the region of repassivation capability after scratch damage for NiTi was, at worst, equivalent to and, at best, ~200 mV potential range greater than SS.

Table 1. Potentiodynamic polarisation test results for NiTi and SS discs in de-aerated (N$_2$ purge) Hank's balanced salt solution

Sample name	E_{corr} mV versus SCE	I_{corr} nA cm^{-2}	CR 10^{-5} mm/year	E_{bd} mV versus SCE
NiTi	−457 (59)[a]	9 (5)[a]	7.85 (4.38)[a]	888 (20)[a]
SS	−265 (33)[b]	9 (1)[a]	8.89 (0.55)[a]	213 (50)[b]

Values are represented in arithmetic mean (standard deviation) format. Superscript letters represent groupings at a 95% confidence level.
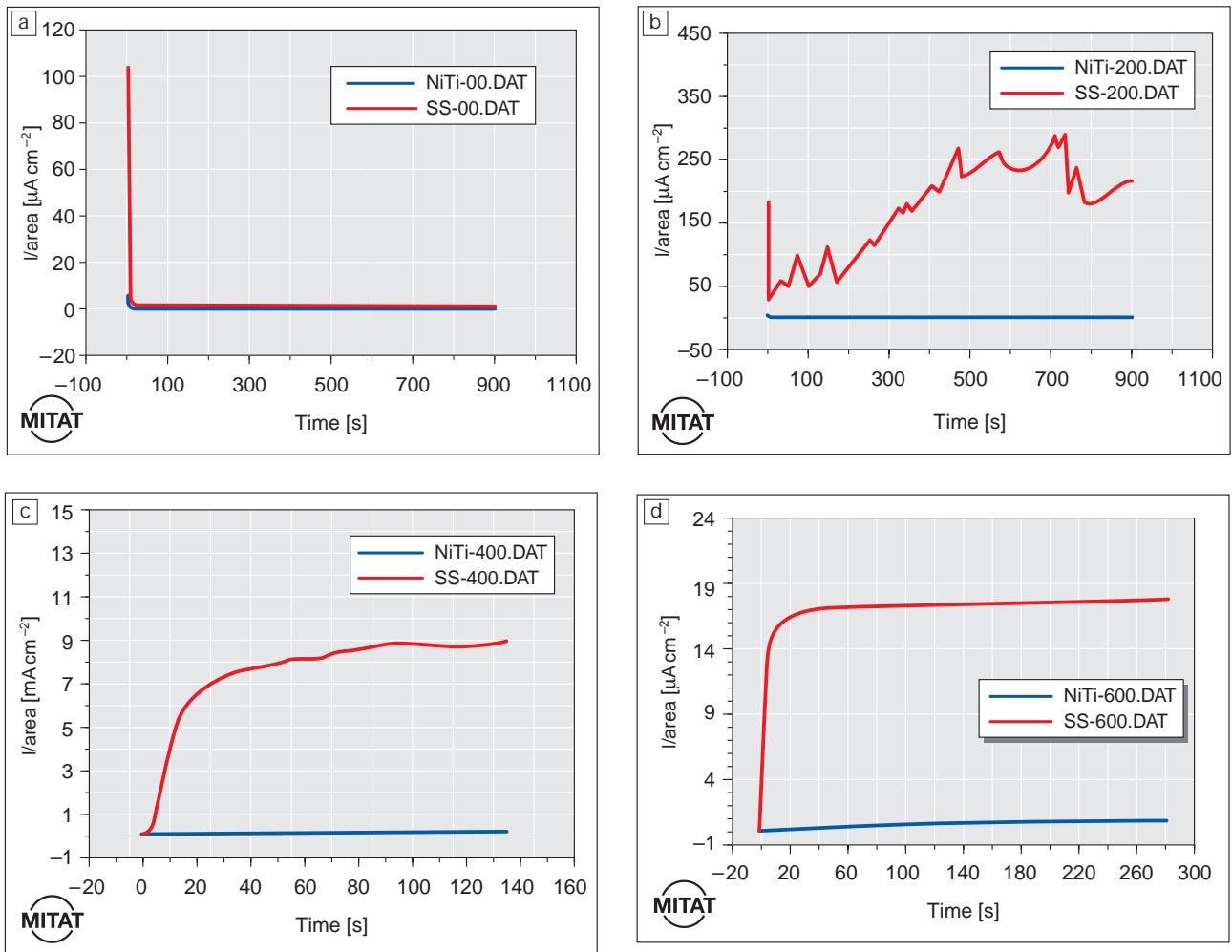
Figure 3. Representative scratch-testing data curves for NiTi and SS in de-aerated Hanks solution at 37°C. Current-density profiles are presented for (a) 0 mV potentiostatic hold, (b) 200 mV potentiostatic hold, (c) 400 mV potentiostatic hold, and (d) 600 mV potentiostatic hold.

In vitro galvanic corrosion behaviour of NiTi

Disc samples of NiTi, platinum (Pt), platinum–iridium alloy (PtIr), gold–palladium alloy (AuPd), SS, tantalum (Ta) and Grade II titanium (Ti) were mechanically polished to 800 grit surface finish using SiC paper. The base-metal alloys were then subjected to passivation treatments based on ASTM F86 protocols for surface preparation of metallic implants. Cyclic polarisation curves obtained for SS and Pt, PtIr, AuPd, Ta and Ti were overlaid with an averaged NiTi curve for mixed-potential theory analysis [21]. The intersection of the cathodic portion of one curve and the anodic portion of the other curve was determined graphically (Figure 4). The y axis intercept was the predicted coupled corrosion potential ($E_{couple-pre}$) and the x axis intercept was the predicted coupled corrosion current density ($I_{couple-pre}$) for that combination [22].

The current-flow ($I_{couple-mes}$) that resulted when the six other materials were galvanically or directly coupled to NiTi alloy (cathode to anode ratio of 1:1) was measured using the potentiostat modified to perform as a zero-resistance ammeter (Technical Notes EG&G, Oak Ridge, TN, 1991). Preliminary testing had determined that the current-density measurements levelled out asymptotically after 6 h, therefore the direct coupling tests were conducted for periods of 12 h. The current density values at t = 12 h represent the asymptotic steady state value of the current flow after an extended period of galvanic coupling. This value may be the most relevant benchmark with reference to a galvanic corrosion scenario for implanted bimetallic devices [21].
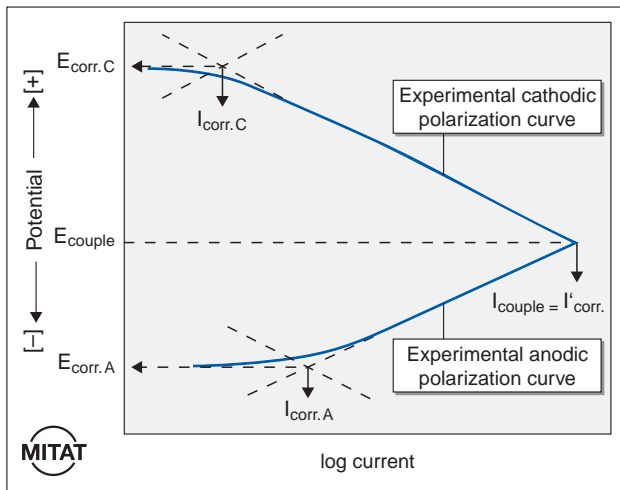
Figure 4. Schematic illustrating mixed-potential theory analysis.

The $E_{couple-pre}$ is indicative of the potential at which a device or a tool made by combining two different materials would rest. If this potential is within the region of corrosion resistance, or lower than the E_{bd} for the individual materials — more specifically the less corrosion-resistant material or anode in the combination, the material combination will not force the anode to corrode at an accelerated rate. The $I_{couple-pre}$ and $I_{couple-mes}$ are the predicted and measured corrosion current density when two materials are combined, respectively. Thus, a higher coupled corrosion current density compared with individual static-corrosion current density (I_{corr}) of the anode would indicate that it would corrode at an accelerated rate. The precision of corrosion measurements is a log decade, or an order of magnitude [23]. Thus, only $I_{couple-mes}$ values an order

of magnitude greater than the I_{corr} can be considered a practically significant increase. Increasing the surface area of the cathode will make the combination more susceptible to galvanic corrosion phenomena.

Consolidated results from mixed-potential theory prediction and the direct coupling experiments are presented in Table 2. Mixed-potential theory calculations predicted that the galvanic coupling of NiTi to:

- Pt and PtIr will result in $E_{couple-pre}$ potentials in the middle of the passive region of the NiTi.
- AuPd and SS will result in $E_{couple-pre}$ potentials in the beginning of the passive region of the NiTi.
- Ta will result in $E_{couple-pre}$ potentials similar to the corrosion potential of the NiTi.

The $I_{couple-pre}$ for NiTi coupled to Pt, PtIr and AuPd was greater than when coupled to Ta. The Tafel regions of NiTi and Ti were too close to each other to conduct tangential extrapolation using mixed-potential theory. The proximity of NiTi and Ti Tafel regions may be indicative of negligible galvanic influence on coupling. The predicted increase in the NiTi corrosion rate when coupled to SS was not conclusive, due to significant standard deviation in the calculated results.

During direct coupling experiments, the largest $I_{couple-mes}$ were obtained for the noble alloys (Pt, PtIr, AuPd) galvanically coupled to NiTi. The smallest $I_{couple-mes}$ values were obtained for SS, Ti and Ta galvanically coupled to NiTi. Also, the $I_{couple-mes}$ values for the (Pt, PtIr, AuPd)/NiTi combinations were an order of magnitude greater than the values for the (SS, Ti, Ta)/NiTi combinations. Good rank order agreement was obtained between the predicted

Table 2. Mixed-potential theory predictions and direct coupling results

Cathode Anode	Mixed potential theory prediction		Direct coupling experiments
	$E_{couple–pre}$ mV versus SCE	$I_{couple–pre}$ nA cm^{-2}	$I_{couple–mes}$ at t = 12 h nA cm^{-2}
Pt–NiTi	126 (22)[a]	277 (9)	836 (74)[a]
PtIr–NiTi	40 (27)[b]	256 (3)	780 (302)[a]
AuPd–NiTi	−137 (3)[c]	285 (2)	608 (34)[a]
SS–NiTi	−218 (76)[d]	176 (111)	35 (5)[b]
Ta–NiTi	−406 (27)[e]	9 (6)	12 (17)[b]
Ti–NiTi	*	*	22 (17)[b]

Values are presented in arithmetic mean (standard deviation) format. Superscript letters represent groupings at a 95% confidence level.
*Predictions could not be made due to proximity of Tafel regions.

results from mixed-potential theory calculations and the results from direct coupling experiments. The increased coupled current density measurements obtained in this study were not of sufficient magnitude to break down the passivated NiTi surface layer due to galvanic action alone. Platt *et al.* galvanically coupled SS to NiTi [24]. Their results did not indicate a statistically-significant increase in current density due to galvanic coupling at a 1:1 cathode to anode ratio. However, they observed localised crevice corrosion phenomena occurring in the SS specimens, while the NiTi specimens remained cathodic or protected. Thus, it is not possible to specifically isolate the galvanic corrosion effects from the crevice corrosion effects for direct comparison with our study.

Platt *et al.* also observed an increase in galvanic activity when they reduced the surface area of the anode by 75%.

In vitro and *in vivo* corrosion of NiTi

Since nickel release during the corrosion of NiTi is an important concern for its use as an implant material, several studies have measured this value. Barrett *et al.* [25] and Bishara *et al.* [26] investigated nickel release from NiTi archwires (processed by the manufacturer) in saliva *in vitro* and reported that NiTi components released an average of 13.05 µg day^{-1}. This value is significantly below the estimated average dietary intake of 200–300 µg day^{-1} [25]. In a second study, orthodontic patients with NiTi appliances had Ni concentration in their blood measured over a period of 5 months [25]. Results showed no significant increase in the nickel blood level throughout this study.

A comparative *in vitro* cell culture study by Ryhänen *et al.* measured Ni released from NiTi and 316L SS in a fibroblast and osteoblast cell culture media [7]. Ni levels were higher in the NiTi group the first day and decreased rapidly as a function of time to achieve similar levels as 316L SS after 8 days in both media. Even though Ni release was higher in the NiTi group, cell proliferation or cell growth near the sample surface was not affected. Also, the NiTi had been only mechanically polished, while the SS had been electropolished according to the guidelines of the manufacturer. Ryhänen *et al.* anticipate a decrease in Ni release if further passivation treatments, such as electropolishing, were performed on the NiTi. Wever *et al.* conducted a similar comparative study with passivated NiTi and SS in Hank's solution [8]. They also found that Ni release from NiTi was maximum the first day (14.5×10^{-7} µg/cm^{-2} sec^{-1}) and reached undetectable levels similar to SS after 10 days.

Castleman *et al.* published the first *in vivo* biocompatibility data on NiTi. They implanted NiTi bone plates in the femurs of beagles for up to 17 months [27]. Retrieved plates exhibited no evidence of either localised or general corrosion. In addition, neutron activation analyses showed no metallic contamination of the surrounding tissues and organs for the NiTi sample group. A recent study by Ryhänen *et al.* investigated implant surface corrosion and systemic trace metal release when NiTi and SS intramedullary rods were implanted in rats for up to 60 weeks [9]. Retrieval analyses exhibited no evidence of localised corrosion on the NiTi implants, while apparent pits were observed on the SS control implants. Also, Ni content analysis of explanted organs did not indicate significant differences between NiTi and SS sample groups.

Conclusions

Passivated Nitinol exhibited increased resistance to primary breakdown of the passive layer and an increased resistance to propagation of existing surface damage compared with 316L SS under static conditions. Passivated Nitinol also exhibited equivalent, if not better ability to repassivate surface damage compared with 316L SS. The galvanic coupling to noble metals or alloys increased the corrosion rate of the Nitinol by two orders of magnitude, while coupling to the base-metal alloys resulted in a corrosion rate in the same order of magnitude as static uncoupled values. The increased current density measurements obtained during direct coupling experiments were not of sufficient magnitude to break down the passivated Nitinol surface layer. Ni release from Nitinol has been shown to be well below dietary levels and decreases rapidly to nearly non-detectable levels in the first few days following Nitinol immersion in a physiological medium. Finally, *in vivo* studies indicate minimal corrosion of Nitinol during implantation, with released nickel concentration in surrounding tissues or organs being equivalent to that released by 316L SS. Thus, carefully passivated Nitinol is a very attractive material for manufacturing minimally-invasive devices and tools.

References

1 Duerig TW, Pelton AR, Stockel D. The utility of superelasticity in medicine. *Bio-Med Mater Eng* 1996; **6:** 255–66.
2 Haasters J, Salis-Solio G, Bonsmann G. The use of

Ni–Ti as an implant material in orthopedics. In: Duerig TW, Melton KN, Stockel D, Wayman CM, editors. *Engineering aspects of shape memory alloys.* Jordan Hill, Oxford: Butterworth-Heinemann, 1990**:**426–44.

3 Lu S. Medical applications of Ni–Ti in China. In: Duerig TW, Melton KN, Stockel D, Wayman CM, editors. *Engineering aspects of shape memory alloys.* Jordan Hill, Oxford: Butterworth-Heinemann, 1990**:** 445–51.

4 Frank TG, Xu W, Cuschieri A. Shape memory applications in minimal access surgery — the Dundee experience. In: Pelton AR, Hodgson D, Russell SM, Duerig T, editors. *Proceedings 2nd International Conference on Shape Memory and Superelastic Technologies (SMST);*Pacific Grove: MIAS, 1997: 509–14.

5 Shabalovskaya SA. On the nature of the biocompatibility and on medical applications of NiTi shape memory and superelastic alloys. *J BioMed Mater Res* 1996;**6:** 267–89.

6 Trepanier C, Leung TK, Tabrizian M, *et al.* Preliminary investigation of the effects of surface treatments on biological response to shape memory NiTi.stents, *J Biomed Mater Res (Appl Biomater)* 1999; **48:** 165–71.

7 Ryhänen J, Niemi E, Serlo W, *et al.* Biocompatibility of nickel–titanium shape memory metal and its corrosion behaviour in human cell cultures. *J BIOMED MATER RES* 1997; **35:** 451–7.

8 Wever DJ, Veldhuizen AG, de Vries J, *et al.* Electrochemical and surface characterization of a nickel–titanium alloy. *Biomaterials* 1998; **19:** 761–9.

9 Ryhänen J, Kalliomen M, Serlo W, *et al.* Bone healing and mineralization, implant corrosion and trace metals after nickel–titanium shape memory metal intramedullary fixation. *JBMR* (in press).

10 Shrier LL, Jarman RA, Burstein OT. *Corrosion–metal/environment reactions*. 3rd edn. Jordan Hill, Oxford: Butterworth-Heinemann, 1995**:** 2**:** 3–2: 164.

11 Park JB, Lakes RS. *Biomaterials: an introduction.* 2nd edn. New York: Plenum Press, 1992: 79–114.

12 Black J. *Biological performance of materials: fundamentals of biocompatibility*. 2nd edn. New York: Marcel Decker, 1992: 38–60.

13 Fontana MG. *Corrosion engineering: modern theory and applications.* 3rd edn. New York: McGraw-Hill, 1986: 445–502.

14 Trepanier C, Tabrizian M, Yahia L'H, *et al.* Effect of the modification of the oxide layer on NiTi stent corrosion resistance, *JBMR (Appl Biomater)* 1998; **43:** 433–40.

15 ASTM F86. Standard practice for surface preparation and marking of metallic surgical implants. In: *Annual book of ASTM standards: medical devices and services*, Vol. 13.01. Philadelphia, PA: American Society for Testing and Materials, 1995: 6–8.

16 Wever DJ, Veldhuizen AG, de Vries J, *et al.* Electrochemical and surface characterization of a nickel–titanium alloy. *Biomaterials* 1998; **19:** 761–9.

17 Trigwell S, Selvaduray G. Effects of surface finish on the corrosion of NiTi alloy for biomedical applications. In: Pelton AR, Hodgson D, Russell SM, Duerig T, editors. *Proceedings 2nd International Conference on Shape Memory and Superelastic Technologies (SMST);*Pacific Grove: MIAS, 1997: 383–8.

18 Venugopalan R, Trepanier C, Pelton AR, Lucas LC. Comparative electrochemical behavior of NiTi and 316L SS. In: The Proceedings of the 25th Annual Meeting of Society for Biomaterials/31st International Biomaterials Symposium, April 28–May 2, 1999, published by Society for Biomaterials, Minneapolis, 7 MN 55441, USA.

19 Rondelli G. Corrosion resistance tests on NiTi shape memory alloy. *Biomaterials* 1996; **17(20):** 2003–8.

20 ASTM Fl46. Standard test method for pitting or crevice corrosion of metallic surgical implant materials. In: *Annual book of ASTM standards: medical devices and services*, vol 13.01 Philadelphia, PA: American Society for Testing and Materials, 1995: 192–7.

21 Venugopalan R, Trepanier C, Pelton AR, Lucas LC: Galvanic corrosion behavior of passivated Nitinol. Accepted for presentation at the World Biomaterials Congress, May 15–May 20, 2000. Proceedings in Press, published by Society for Biomaterials, Minneapolis, 7 MN 55441, USA.

22 Jones DA. *Principles and prevention of corrosion.* 2nd edn. Upper Saddle River, NY: Prentice Hall, 1996: 168–98.

23 ASTM G61: Standard test method for conducting cyclic potentiodynamic polarization measurements for localized corrosion susceptibility of iron-, nickel-, or cobalt-based aloys. In: *Metals, test methods and analytical procedures*, Vol 03.02. Philadelphia, PA: American Society for Testing and Materials, 1995: 224–8.

24 Platt JA, Guzman A, Zuccari A, *et al.* Corrosion behavior of 2205 duplex stainless steel. *Am J Orthod Dentofac Orthop* 1997; **112:** 69–79.

25 Barrett RD, Bishara SE, Quirin JK. Biodegradation of orthodontic appliances. Part 1. Biodegradation of nickel and chromium *in vitro. Am J Orthod Dentofac Orthop* 1993; **103:** 8–14.

26 Bishara SE, Barrett RD, Selim MI. Biodegradation of orthodontic appliances. Part II, Changes in the blood level of nickel. *Am J Orthod Dentofac Orthop* 1993; **103:** 115–9.

27 Castleman LS, Motzkin SM, Alicandti SM, Bonawit VL. Biocompatibility of nitinol alloy as an implant material. *JBMR* 1976; **10:** 695–731.